



ELSEVIER

Tectonophysics 323 (2000) 163–182

**TECTONOPHYSICS**

www.elsevier.com/locate/tecto

# Miocene rotations in the Eastern Alps — palaeomagnetic results from intramontane basin sediments

Emő; Márton <sup>a,\*</sup>, Joachim Kuhlemann <sup>b</sup>, Wolfgang Frisch <sup>b</sup>, István Dunkl <sup>b</sup>

<sup>a</sup> *Eötvös Loránd Geophysical Institute of Hungary, Paleomagnetic Laboratory, Columbus u. 17–23, 1145 Budapest, Hungary*

<sup>b</sup> *Institut für Geologie und Paläontologie, Universität Tübingen, Sigwartstraße 10, 72076 Tübingen, Germany*

Received 22 June 1999; accepted for publication 25 March 2000

## Abstract

A palaeomagnetic study of late Early Miocene to late Middle Miocene sediments from the Eastern Alpine intramontane basins revealed counterclockwise rotations in the Ennstal, in the western part of the Noric and in the Lavanttal depressions. For the basal strata of the basins, declinations are between 273° and 315°, while for the younger strata they are between 321° and 333°, in perfect agreement with observations from the Klagenfurt basin. The results suggest syndepositional rotation during the lateral tectonic extrusion of the Eastern Alps (ca. 17–13 Ma), which was also responsible for the formation of the mostly transtensional basins. We propose a model in which domino-shaped blocks, separated by NNW–SSE trending dextral faults, rotated counterclockwise due to faster eastward motion in the south relative to areas further north. The protrusion of the Bohemian spur inhibited eastward motion in the northern part of the study area, thus creating a sinistral wrench corridor. After lateral extrusion had ceased the counterclockwise rotation continued probably as ‘en bloc’ rotation of ca. 30°. Clockwise rotation was observed in the eastern part of the Noric depression, which appears to belong to a limited area with complex rotation pattern near the eastern margin of the Alps. This area is wedged between the counterclockwise rotated Eastern Alps and the similarly rotated North Pannonian area in Hungary. © 2000 Elsevier Science B.V. All rights reserved.

*Keywords:* Eastern Alps; intramontane basins; Miocene; palaeomagnetism; tectonic model

## 1. Introduction

In the last decade several palaeomagnetic studies reported Tertiary, mainly Miocene rotations from the surroundings of the Eastern Alps (e.g. Márton and Márton, 1996; Márton et al., 1996; Vass et al., 1996; Fodor et al., 1998; Kempf et al., 1998; Márton et al., 1999a,b).

From the Eastern Alps, however, very few palaeomagnetic data are published which may be

regarded as indicative of Tertiary rotations. Most of them were obtained on metamorphic rocks and interpreted as overprint magnetizations of Tertiary age (Mauritsch et al., 1991; Burgschwaiger et al., 1996), others were observed on Gosau sediments of late Cretaceous age (Agnoli et al., 1989) and consequently, the counterclockwise rotation they exhibited was attributed to Tertiary movements (Márton and Mauritsch, 1990).

The lack of direct evidence for the very likely rotations that must have accompanied Miocene lateral extrusion in the Eastern Alps (Ratschbacher et al., 1991) was the reason why we started a systematic palaeomagnetic study on the sediments

\* Corresponding author. Tel./fax: +36-1-319-3203.  
E-mail address: h11000mar@ella.hu (E. Márton)

of the intramontane basins. Our aim was to quantify the movements and constrain the timing of the rotations.

## 2. Geological background

The Eastern Alps are dominated by the Austroalpine mega-unit (Fig. 1), which represents the rigidly behaving upper plate during Early Tertiary continental collision. The Austroalpine unit acted as an orogenic lid above the Penninic mega-unit, which contains remnants of the Neo-Tethys ocean separating the Austroalpine unit (a former part of the Africa-derived Adriatic plate), and the European plate (e.g. Frisch, 1979; Dercourt et al., 1985). The Penninic domain was rapidly exhumed in Miocene times, forming meta-

morphic dome structures, which are exposed in windows (Fig. 1; Frisch et al., 1998).

The object of the present study is the area east of the Tauern window, where the Austroalpine megaunit comprises the crystalline basement, weakly metamorphosed Palaeozoic sequences and subordinate Permian and Mesozoic cover sequences (Figs. 1 and 2). The Penninic windows to the east (Rechnitz window) and west (Tauern window) of this area indicate that the Austroalpine domain floats on the Penninic substratum. Seismic measurements suggest that the Austroalpine/Penninic boundary reaches a maximum depth of ca. 10 km between these windows (Aric et al., 1987; Ratschbacher et al., 1991).

Early Tertiary continental collision was responsible for the formation of a thickened crustal stack. Thermal weakening of the crust with  $T_{max}$  ca.

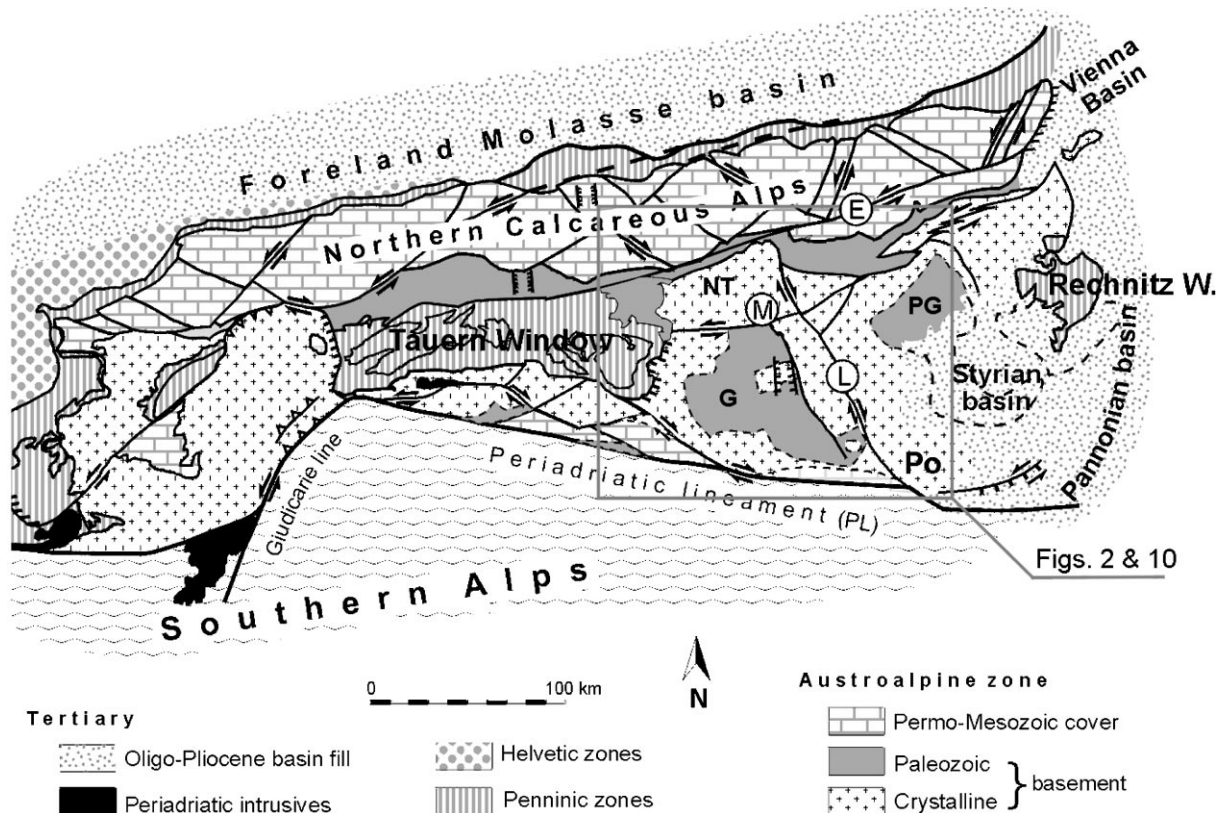


Fig. 1. Tectonic framework of the Eastern Alps. E, Ennstal fault; M, Mur-Mürztal fault (Noric depression); L, Lavanttal fault; Po, Pohorje mountains; NT, Niedere Tauern; G, Gurktal Alps; PG, Palaeozoic of Graz.

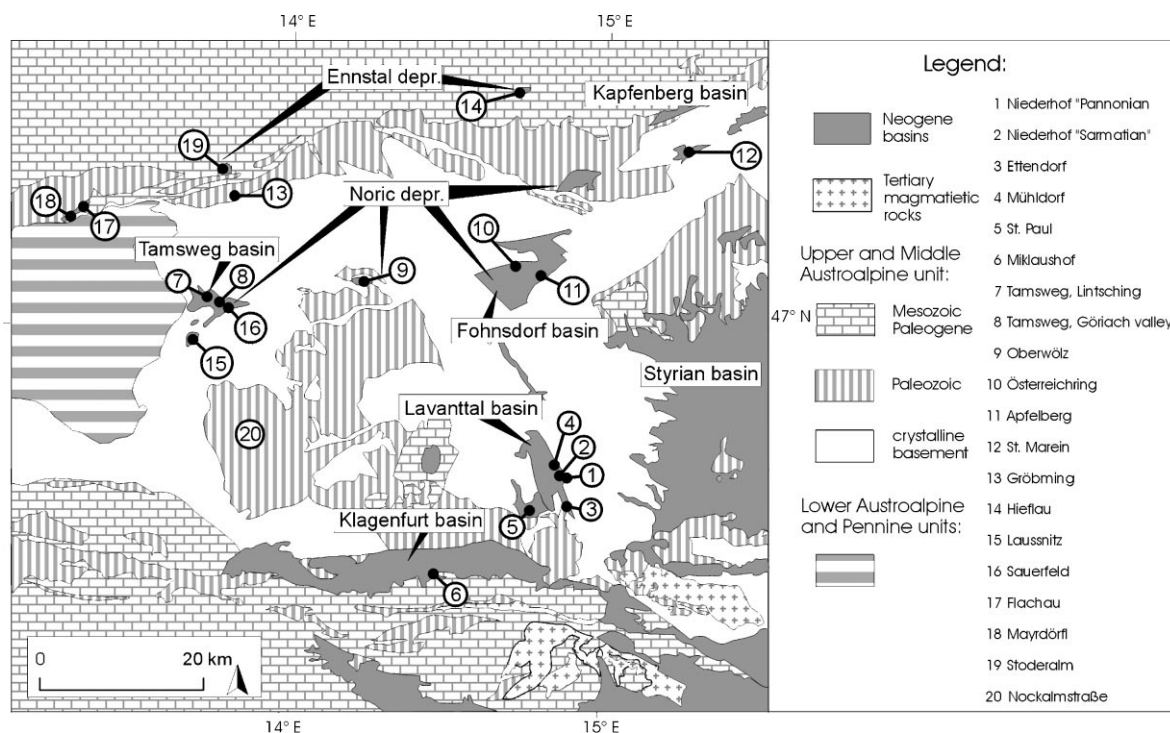


Fig. 2. Geologic framework of the study area with the sampling localities. Numbers refer to Tables 1–4 and are used throughout the text.

30 Ma (Christensen et al., 1994) and Oligocene uplift of the Alps, west of the later Tauern window (Frisch et al., 1998) formed the prerequisites for gravity-driven orogenic collapse in Early and Middle Miocene times (Ratschbacher et al., 1991). Around 17 Ma, when exhumation rates in the metamorphic domes of the Tauern window may have attained values on the order of  $5 \text{ mm yr}^{-1}$  (Cliff et al., 1985), the Austroalpine lid disintegrated into a number of tectonic blocks that moved eastward on top of the softened Penninic substratum and along large-scale strike-slip faults. The combination of orogen-parallel collapse and block escape was described as 'lateral tectonic extrusion' by Ratschbacher et al. (1991).

Transtensional movement along large-scale conjugate strike-slip fault zones created a number of short-lived intramontane basins filled with Oligocene or Karpatian through Badenian (for correlation with Mediterranean stages see Fig. 3)

sediments. Most of the basins represent pull-apart or negative flower structures along the sinistral Ennstal, the sinistral Mur-Mürztal ('Noric depression'), and the dextral Lavanttal fault systems (Figs. 1 and 2).

The sediment fill of the basins is not metamorphosed, the age of the deposition is poorly constrained by palaeontological data (Table 1). Nevertheless, it is generally accepted that the climax of subsidence and sedimentation in the different basins was synchronous, that is, in the time span between 18 and 15 Ma (Weber and Weiss, 1983; Tollmann, 1985). Younger sediments than 15 Ma occur in the Lavanttal (up to 10 Ma) and in the Klagenfurt basins. The latter is a relatively large, asymmetric basin, where sedimentation started in Sarmatian times (ca. 12 Ma). The formation of this basin was probably related to the eastward extrusion of the Bakony escape block (Frisch et al., 1998).

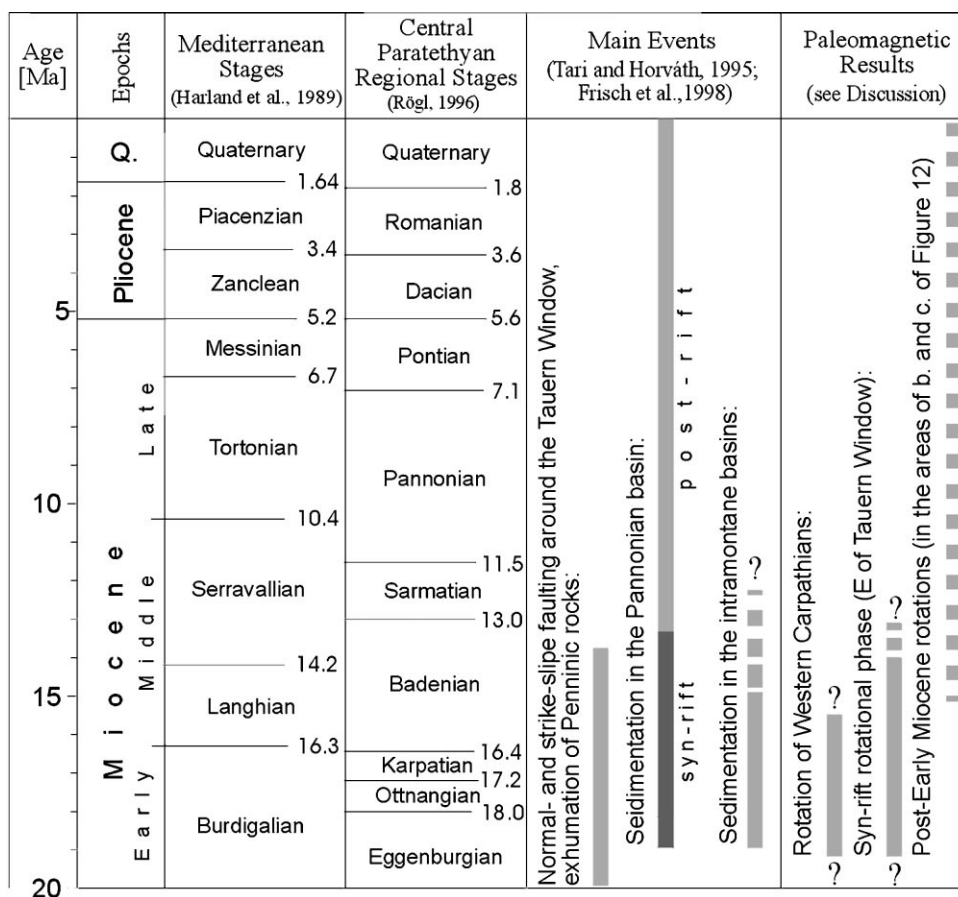


Fig. 3. Time scale with the Mediterranean (Harland et al., 1989) and Paratethyan (Rögl, 1996) stages and the major structural, sedimentological (Tari and Horváth, 1995; Frisch et al., 1998) and palaeomagnetic (Márton and Márton, 1996; Márton et al., 1996; Túnyi and Márton, 1996; Márton et al., 1998, 1999a) events.

### 3. Sediments of the intramontane basins and palaeomagnetic sampling

The intramontane basins contain conglomerates, sandstones, siltstones, claystones and marls (Tollmann, 1985, and references therein). Conglomerates are generally dominant in the basal parts of the sequences and are derived from local sources. Coal seams and layers are frequent in the Miocene sediment pile. In fully preserved profiles, sandy to clayey or marly materials dominate, representing low-energy fluvial and lacustrine environments. In the latter, turbidites are common. It is only in the Lavanttal basin where marine deposits are present. The intramontane basins are lined up

along valley-like depressions. However, there are some Miocene occurrences in uplifted position that are considered as having been continuous with the valley-fills nearby [e.g. locality 19 situated 1000 m above the valley floor in the eastern Dachstein massif with locality 13 in the valley or locality 15 uplifted 700 m above the Tamsweg basin with localities 7, 8 and 16 in the basin itself (Fig. 2)].

#### 3.1. Ennstal depression

The formation ages of the basin remnants related to the Ennstal fault system (Fig. 2) are estimated through correlation with other basins and palaeogeographic reconstructions. Thus, the

Table 1  
Basic geographical and geological data of the palaeomagnetic sampling localities

No.	Locality	Age <sup>a</sup>	Reference for age	Map no./name	YM31-450 <sup>b</sup>	XGKM <sup>b</sup>	Elevation (m)	Sample colour	Oxidation colour	Grain size	Structures
1	Niederhof uphill	Pannonian	Beck-Mannagetta (1952)	205 St. Paul i.L.	642850	173550	450	Grey	Yellow	Silty clay	Poorly stratified
2	Niederhof valley	Sarmatian	Beck-Mannagetta (1952)	205 St. Paul i.L.	642630	172800	395	Grey	Yellow	Clayey silt	Flaser bedding
3	Ettendorf	L. Badenian	Beck-Mannagetta (1952)	205 St. Paul i.L.	644570	169600	370	Dark brown	–	Clayey silt	Stratified to laminated
4	Muehldorf	E. Badenian	Papp (1957); Schmid (1974)	205 St. Paul i.L.	637750	178700	395	Dark grey	–	Silty clay	Strongly biotubated
5	St. Paul	?Otn.-Karp.	Klaus, 1956	204 Völkermarkt	562770	172850	550	Red	Yellow	Silty clay	Poorly stratified
6	Miklaushof	L. Sarmat.	Papp (1957)	204 Völkermarkt	549500	156350	570	Red to green	Yellow	Clayey silt	Stratified
7	Tamsweg, Lintsching	L. Karpatian	Heinrich (1978)	157 Tamsweg	482790	223650	1100	Dark brown	–	Clayey silt	Stratified to laminated
8	Tamsweg, Göriach	L. Karpatian	Heinrich (1978)	157 Tamsweg	484050	224040	1095	Brown	–	Marly silt	Flaser bedding
9	Oberwölz	Karpatian?	Tollmann (1985)	159 Murau	522860	229400	920	Red	–	Silt-fine sand	Stratified
10	Österreichring	Karpatian	Mottl (1970); Polesny (1970)	161 K nittelfeld	558600	232550	710	(Dark) grey	–	Clayey sand	Stratified
11	Knittelf./Apfelberg	E. Badenian	Mottl (1970); Polesny (1970)	162 K öflach	637030	229250	695	Dark grey	–	Clayey silt	Stratified
12	St. Marein	Karpatian	Weber and Weiss (1983)	134 Passail	675850	258300	555	Dark grey	–	Clayey silt	Laminated
13	Gröbming	?Karpatian	Sachsenhofer (1988)	128 Gröbming	497400	260870	705	Grey	Brown	Clayey sand	Poorly stratified
14	Hieflau	?Otn.-Karp.	Wagreich et al. (1996)	100 Hieflau	559720	274150	810	Grey	–	Silty clay	Stratified
15	Bonner Hütte	Karpatian	Zelinger et al. (1999)	157 Tamsweg	476030	210870	1675	Dark grey	Brown	Silty clay	Poorly stratified
16	Sauerfeld	Karpatian	Heinrich (1978)	158 Stadl./Mur	489100	222220	1100	Grey	–	Silty sand	Stratified
17	Flachau/sawmill	?Karpatian	Sachsenhofer (1988)	126 Radstadt	452250	246400	915	Dark grey	–	Pebbly silt	Poorly stratified
18	Mayrdörfel/ski-lift	?Karpatian	Sachsenhofer (1988)	126 Radstadt	450380	245820	1140	Dark grey	–	Silty sand	Poorly stratified
19	Stoderalm	?Otn.-Karp.	Frish et al. (1998)	127 Schladming	487350	258650	1680	Olive-grey	Brown	Silty sand	Poorly stratified
20	Nockalmstraße	Mesoz. dike	Balogh, personal communication	183 Radenthein	487200	195058	1540	Grey	Brown	Silty clay, sand	Poorly stratified

<sup>a</sup> Otnangian (Otn), Karpatian, Badenian, Sarmatian, Pannonian are Central Paratethyan regional stages. For correlation with Mediterranean stages consult Fig. 3.

<sup>b</sup> Rechtswert and Hochwert in the Gauss–Krueger coordinates of Austrian ÖK 50 000 sheets.

age assigned to the (coal-bearing) sandstones, claystones and marls of localities 19, 13 and 14 is Ottungian–Karpatian, localities 17 and 18 are of Karpatian age (Table 1).

### 3.2. Noric depression

In the western part of the Noric depression (Upper Murtal) and in the related uplifted occurrence Karpatian sediments were sampled (Fig 2). These were pockets of grey claystones found in gravel (locality 15), grey-brown siltstone, with graded bedding, deposited in lacustrine environment (locality 8), marl (locality 7), a siltstone layer within the basal conglomerates (locality 16), and reddish to yellowish clayey siltstone which forms lenses and pockets in a thick conglomerate sequence (locality 9).

In the Fohnsdorf basin (Fig. 2) which is situated at the junction of two important conjugate fault zones, two localities were sampled, one below and one above a local unconformity: below the unconformity lacustrine marly material of Karpatian age (locality 10), above the unconformity, several silty-sandy horizons from a thick Badenian sequence of immature sandstones and conglomerates (locality 11).

In the eastern part of the Noric depression (Mürztal) several silty horizons with different tilt angles were sampled from a Karpatian sequence (locality 12, Fig. 2).

### 3.3. Lavanttal basin

The Lavanttal basin is a transtensional feature including pull-apart and halfgraben structures following the NNW–SSE trending Lavanttal fault system (Fig. 2). The Granitztal subbasin was formed prior to the main basin and shows an elongation perpendicular to it.

From the Granitztal subbasin a terrestrial silty clay was sampled (locality 5). From the Lavanttal basin fossiliferous, silty clays of Badenian age (localities 3 and 4), Late Sarmatian clayey silt (locality 2) and Pannonian claystones and marls (locality 1) were collected.

### 3.4. Klagenfurt basin

Though the Klagenfurt basin is a large one (75 km long), outcrops are scarce, and secondary oxidation is widespread. Thus, only one locality was sampled from this basin, a claystone of Sarmatian age (locality 6).

## 4. Laboratory measurements and results

In the Paleomagnetic Laboratory of Eötvös Loránd Geophysical Institute (ELGI) standard-size specimens were cut from the drill cores. Natural remanent magnetization (NRM) of each specimen were measured using either a two-axis

Table 2  
Palaeomagnetic results: Ennstal depression

Locality	Number of used/ collected samples	$D^\circ$	$I^\circ$	$k$	$\alpha_{95}^\circ$	$D_C^\circ$	$I_C^\circ$	$k$	$\alpha_{95}^\circ$	Dip	Remarks
19 Stoderalm AH 361–380	11/20	<b>356</b>	<b>+57</b>	42	7	–	–	–	–	340/44	c
13 Gröbming	A 7	<b>305</b>	<b>+51</b>	13	18	302	–13	13	18	295/65	a
AH 262–275	B 7	302	–40	13	14	<b>275</b>	<b>+74</b>	13	14		
17 Flachau AH 346–352	6/7	<b>93</b>	<b>–54</b>	16	17	(31)	(–51)	16	17	155/43	c
14 Hieflau	A 5	<b>342</b>	<b>+61</b>	75	9	295	+41	75	9	255/40	a
AH 276–286	B 4	45	+59	24	19	<b>306</b>	<b>+71</b>	24	19		
Subtracted vectors 150–250°C	A 7/8	337	+67	53	8	–	–	–	–		

In most cases where the number of samples used is less than that of the collected, the samples omitted disintegrated during cutting or demagnetization and measurement. Exceptions are locality 9, where the samples omitted had extremely weak NRMs, and locality 11, where instability on demagnetization accounts for rejection.

$D$ ,  $I$  and  $D_C^\circ$ ,  $I_C^\circ$ , mean palaeomagnetic declination, inclination before and after tilt correction.  $k$  and  $\alpha_{95}^\circ$ : statistical parameters (Fisher, 1953).

Remarks: a=results of component analysis (Kent et al., 1983); b=combination of stable end points and remagnetization circles (McFadden and McElhinny, 1988); c=last meaningful demagnetization step.

Table 3

Palaeomagnetic results: Noric depression, Lausnitz occurrences and Gurktal block

Locality	Number of used/ collected samples	$D^\circ$	$I^\circ$	$k$	$\alpha_{95}^\circ$	$D_C^\circ$	$I_C^\circ$	$k$	$\alpha_{95}^\circ$	Dip	Remarks
<b>Noric depression</b>											
<i>Tamsweg basin</i>											
8 Göriach valley											
AH 81–89	9/9	139	–71	200	4	134	–54	200	4	308/17	c
AH 213–219	7/7	199	–72	129	5	159	–62	129	5	298/19	a
AH 220–226	3/7	127	–63	89	13	124	–44	89	13	298/19	a
Göriach valley	19/25	156	–72	43	5	<b>141</b>	– <b>56</b>	52	5		
7 Building site AH 103–118	15/16	332	+68	12	11	<b>331<sup>a</sup></b>	+ <b>64<sup>a</sup></b>	42	6	Variable	a
<i>Obervöltz basin</i>											
9 Obervöltz AH 205–212 227–238	9/18	285	66	19	12	<b>296</b>	+ <b>51</b>	19	12	314/16	a
5 pockets											
<i>Fohnsdorf basin</i>											
11 Apfelberg AH 39–68, 287–292	4/36	53	+37	32	16	<b>66</b>	+ <b>54</b>	32	16	204/21	c
<i>Kapfenberg–St. Marein basin</i>											
12 St. Marein											
AH 1–7	7/8	311	–65	84	7	<b>236</b>	– <b>56</b>	84	7	14/39	a
AH 8–16	7/9	313	–64	141	5	<b>238</b>	– <b>56</b>	141	5	14/39	a
AH 17–24	7/8	171	–24	48	9	163	+40	48	9	26/78	c
AH 25–29	5/5	190	+9	21	17	125	+74	21	17	26/78	c
AH 30–38	7/9	164	–11	32	11	120	+57	32	11	17/95	c
St Marein	5 (29) <sup>a</sup>	–	–	–	–	<b>248</b>	– <b>52</b>	33	15		b
<b>Lausnitz occurrences</b>											
15 Bonner Hütte AH 320–333	9/14	<b>289</b>	+ <b>45</b>	15	14	295	+35	15	14	330/12	c
<b>Gurktal block</b>											
20 Nockalmstraße AH 313–319	6/7	112	–43	118	6	<b>112</b>	– <b>43</b>	118	6	–	a

In most cases where the number of samples used is less than that of the collected, the samples omitted disintegrated during cutting or demagnetization and measurement. Exceptions are locality 9, where the omitted samples had extremely weak NRM, and locality 11, where instability on demagnetization accounts for rejection.

$D$ ,  $I$  and  $D_C^\circ$ ,  $I_C^\circ$ , mean palaeomagnetic declination, inclination before and after tilt correction.  $k$  and  $\alpha_{95}^\circ$ : statistical parameters (Fisher, 1953).

Remarks: a=results of component analysis (Kent et al., 1983); b=combination of stable end points and remagnetization circles (McFadden and McElhinny, 1988); c=last meaningful demagnetization step.

<sup>a</sup> Number of sites (samples) used; statistic is based on sites.

cryogenic magnetometer, or JR-4 spinner magnetometers and susceptibility with a KLY-2 susceptibility bridge. One or two specimens per sample were demagnetized in increments by alternating field (AF), thermal method, or a combination of the two, until the magnetic signal was lost. As a result, characteristic remanence was isolated for the localities shown in Tables 2–4

#### 4.1. Magnetic minerals

The general characteristic of the NRM is moderate stability on thermal demagnetization.

Isothermal remanent magnetization (IRM) acquisition curves in such cases exhibit low coercivity magnetic mineral, which may be magnetite (maghemite) and/or iron sulphides (Fig. 4, samples AH 270A, AH 225B, AH 18A). Thermal demagnetization of the three-component IRM (method by Lowrie, 1990) as well as that of the NRM, and the behaviour of susceptibility on heating, both measured at room temperature after each demagnetization step or on continuous heating in a low magnetic field (Fig 5, AH 276 and AH 142) point to iron sulphides (with or without magnetite) as the magnetic mineral. There are only three locali-

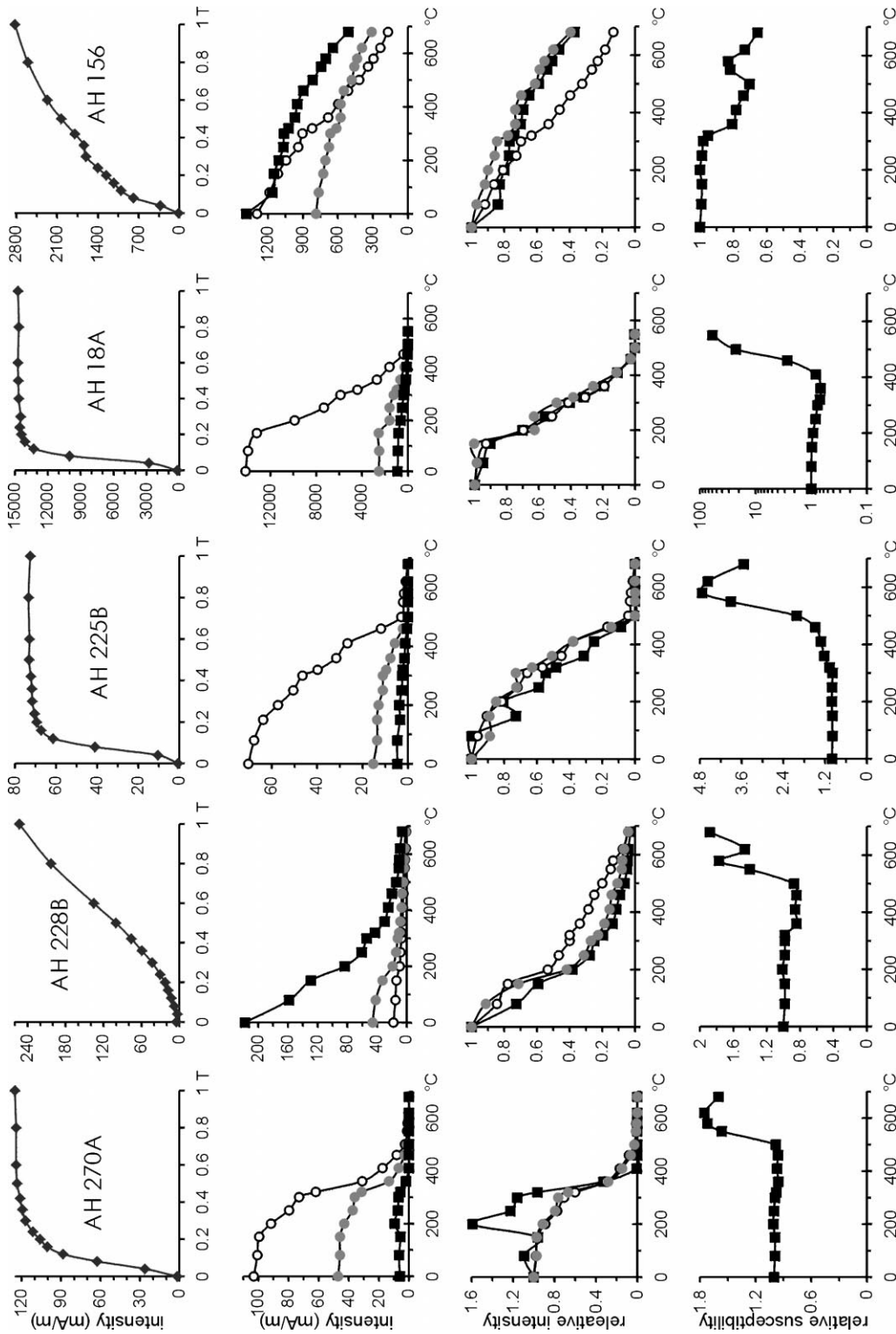


Fig. 4. Identification of the magnetic minerals. From top to bottom, IRM acquisition curves, thermal demagnetization of the tree-component IRM, same normalized, normalized susceptibility versus temperature curve. Examples are from localities 13 (AH 270A), 9 (AH 228B), 8 (AH 225B), 12 (AH 18) and 5 (AH 156). Key to the three component demagnetization curves: open circles, soft component; grey symbols, medium hard component; black symbols, hard component. The components were acquired in magnetic fields of 0.20, 0.36 and 1.00 T, respectively.

Table 4  
Palaeomagnetic results: Lavanttal and Klagenfurt basin

Locality	Number of used/ collected samples	$D^\circ$	$I^\circ$	$k$	$\alpha_{95}^\circ$	$D_C^\circ$	$I_C^\circ$	$k$	$\alpha_{95}^\circ$	Dip	Remarks
<b>Lavanttal</b>											
5 W of St. Paul AH 152–167	11/16	333	+58	36	8	<b>314</b>	<b>+52</b>	36	8	258/15	a
4 Mühldorf AH 119–129, 130–135	11/17	<b>332</b>	<b>+61</b>	35	8	324	+26	35	8	314/36	a
2 Niederhof AH 136–147	7/12	<b>333</b>	<b>+54</b>	30	11	325	+53	30	11	247/6	a
<b>Klagenfurt basin</b>											
6 Miklaushof AH 168–175	6/8	<b>336</b>	<b>+62</b>	44	10	343	+44	44	10	56/4	a

In most cases where the number of samples used is less than that of the collected, the samples omitted disintegrated during cutting or demagnetization and measurement. Exceptions are locality 9, where the omitted samples had extremely weak NRMs, and locality 11, where instability on demagnetization accounts for rejection.

$D$ ,  $I$  and  $D_C^\circ$ ,  $I_C^\circ$ , mean palaeomagnetic declination, inclination before and after tilt correction.  $k$  and  $\alpha_{95}^\circ$ : statistical parameters (Fisher, 1953).

Remarks: a=results of component analysis (Kent et al., 1983).

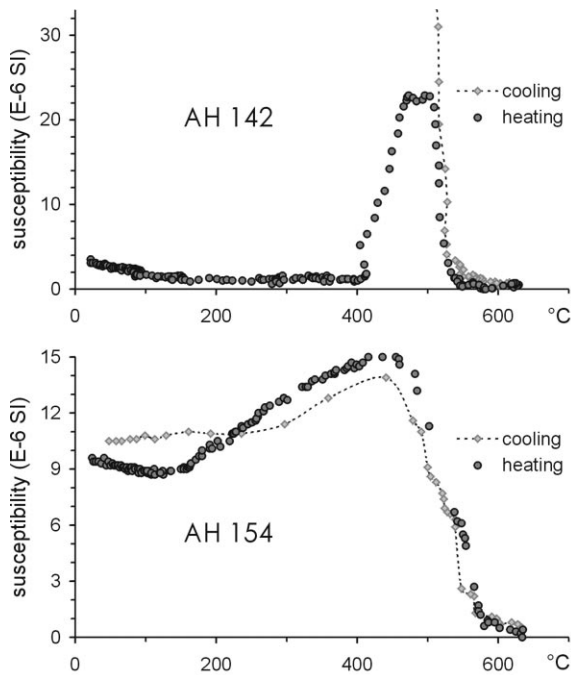


Fig. 5. Identification of magnetic minerals. Low-field susceptibility versus temperature curves. Examples are from localities 2 (AH 142) and 5 (AH 154), respectively.

ties (5, 9 and 17) where the presence of iron sulphides can be excluded and the iron is in high oxidation state. At locality 5 magnetite and hematite (Fig. 4, AH 156 and Fig. 5, AH 154), while at

locality 9 hematite and goethite (Fig. 4, AH 228) are observed. The samples from locality 17 may contain hematite or oxidized magnetite, but identification of the carrier is difficult due to the steep increase of the susceptibility on heating above 580°C.

#### 4.2. Anisotropy of magnetic susceptibility

Anisotropy of the magnetic susceptibility (AMS) was measured for all localities, except 15 and 19. The results may be summarised as follows.

The degree of anisotropy is typically 2–5%. Where it is <2% (locality 9 and site AH 30–38 at locality 12) the magnetic fabric is unoriented; When it is higher, the minima cluster close to the bedding pole.

The degree of lineation is typically <2%. Clustering of the minima and intermediate susceptibility directions is observed at some localities (sites AH 8–16 and AH 17–24 at locality 12, all sites at locality 10, 11, 13, 16 and 18. Note that locality 10, 16, 18 and most sites at locality 11 did not yield palaeomagnetic directions). Orientation of the magnetic particles by water-current or incipient deformation can explain the grouping of the maxima.

In summary, the magnetic fabric of the sediments of the intramontane basins of the Eastern Alps is that of an undeformed or slightly deformed

rock and both the degree of foliation and lineation is so low, that bias in the direction of the magnetic vector from the direction of the ambient Earth's magnetic field is highly unlikely.

#### 4.3. Palaeomagnetic directions

In general, site and locality mean remanence directions (Tables 2–4) are characterized by excellent to acceptable statistical parameters. Different authors set different limits to what is acceptable. Irving (1964) draws the upper limit for  $\alpha_{95}$  at  $25^\circ$ , while more recently van der Voo (1993) at  $16^\circ$ . In Tables 2–4, it is only one of the components for localities 13 and 14 and the locality mean for 17 which do not satisfy the more rigorous criterion. Nevertheless, their  $\alpha_{95}$  is well below the less rigorous limit, thus they are also used in the final tectonic interpretation.

Before tilt correction, the mean palaeomagnetic directions differ (except locality 19) from that of

the present Earth's magnetic field. The age of the magnetization with respect to tilting is a matter of consideration, since fold test at outcrop level is not possible.

From the *Ennstal depression* four localities yielded characteristic magnetizations (Table 2). The mean direction for locality 19 is that of the present Earth's magnetic field in the geographic coordinate system. The result is, therefore, of no value for tectonic interpretation. Localities 13 and 14 are characterized by two magnetic components (Fig. 6a), component B is interpreted to be of pre-, component A of post-tilting age (Table 2). The NRM of the samples from locality 17 was extremely hard on AF demagnetization; thermal demagnetization in increments was successful in improving statistical parameters (before demagnetization  $D=87^\circ$ ,  $I=-43^\circ$ ,  $k=7$ ,  $\alpha_{95}=25^\circ$ ), but the intensity of the NRM was hardly reduced at  $580^\circ\text{C}$ , the last step of demagnetization, before the susceptibility dramatically increased (Fig. 6b) or

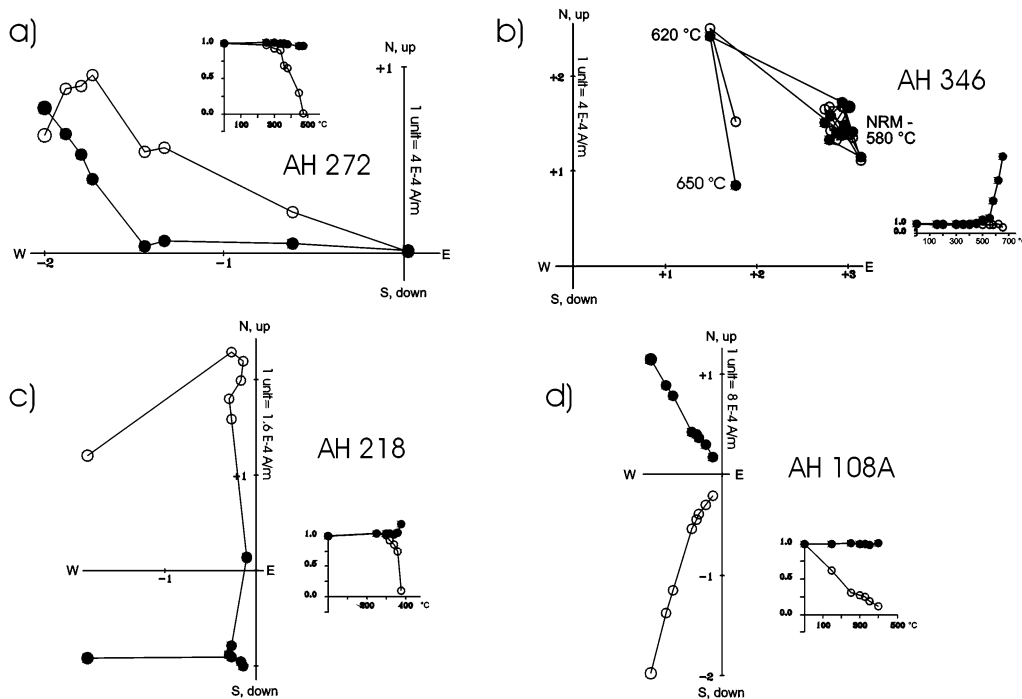


Fig. 6. Typical demagnetization curves in the geographic system from the Ennstal and the western part of the Noric depressions. The behaviour of the NRM on stepwise thermal demagnetization (Zijderveld plots, filled symbols projection of the magnetic vector in the horizontal plane; open symbols, the same in a vertical plane) and normalized susceptibility (dots)/intensity (circles) versus temperature curves. Examples are from localities 13 (a), 17 (b), 8 (c) and 7 (d).

the physical disintegration of the samples. The mean direction was calculated from the NRM measured after 580°C.

In the western part of the *Noric depression* localities 7 and 8 (Tamsweg basin) are characterized by good demagnetization curves (Fig. 6c and d) and yielded statistically well defined palaeomagnetic directions (Table 3). The sediment of locality 15 exhibits fairly stable behaviour of the NRM on both heating and AF demagnetization, but becomes unstable before the signal is lost. From locality 9 several samples were too weakly magnetic. Those with stronger NRM signal (in the range of  $10^{-4}$  A m<sup>-1</sup>) retained some of the NRM after the goethite was eliminated and served to define the locality mean direction in Table 3.

The majority of the samples collected from the

*Fohnsdorf basin* (localities 10, 11) were unstable. It was only one site (four samples) from locality 10 which yielded acceptable direction.

The eastern part of the *Noric depression* is represented by locality 12 where all five sites yielded good palaeomagnetic signals (Fig. 7a and b). The mean directions of two of them (AH 1-7, AH 8-16) are in excellent agreement. The other three sites behave similarly during demagnetization, that is, the NRMs move along great circles (Fig. 8), so the remanence measured after the last meaningful demagnetization step may still be a composite NRM. The great circles in the tectonic coordinate system go through or pass very close to the site mean directions (also in the tectonic coordinate system) of the first two sites. Using the combination of stable end points (site mean direc-

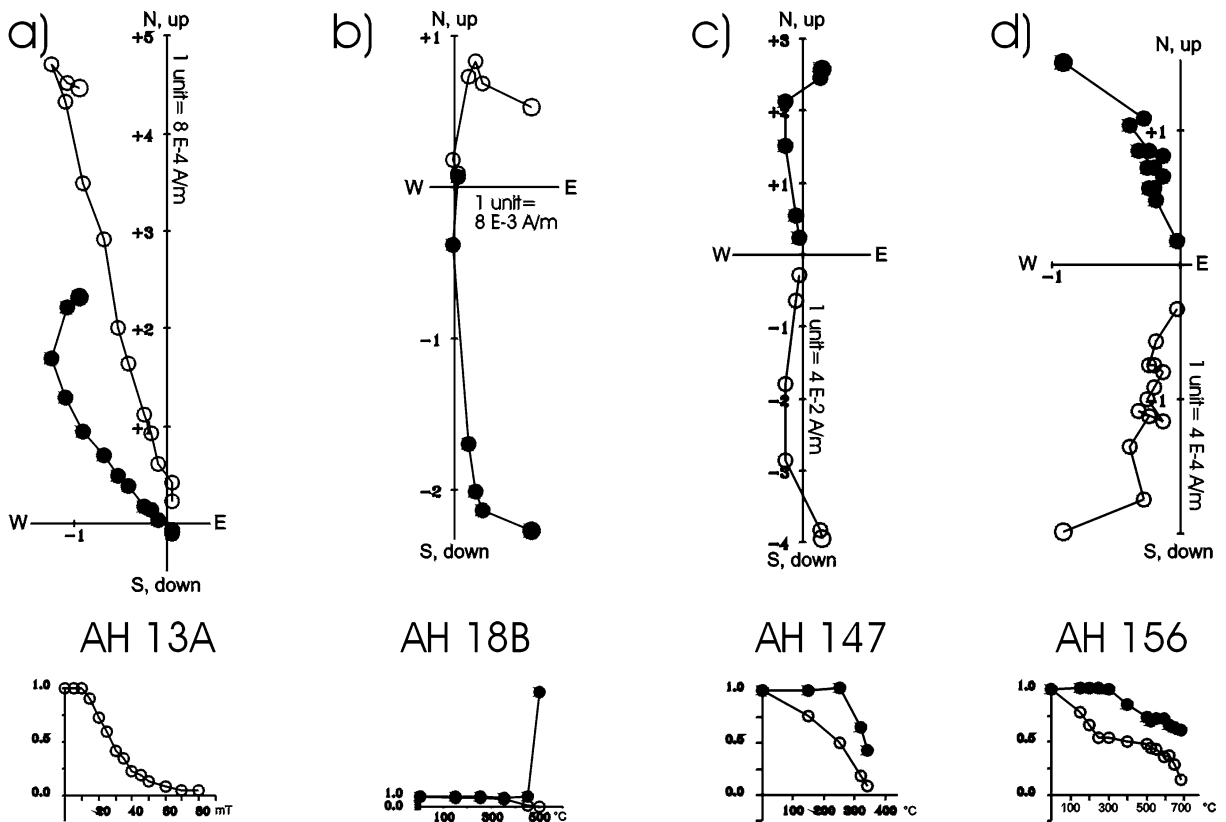


Fig. 7. Typical demagnetization curves in the geographic system from the eastern part of the Noric depression and the Lavantal–Graniztal basins. The behaviour of the NRM on stepwise thermal (AF for 7a) demagnetization (Zijderveld plots: filled symbols, projection of the magnetic vector in the horizontal plane; open symbols, the same in a vertical plane) and normalized susceptibility (dots)/intensity (circles) versus temperature curves. Examples are from localities 12 (a and b), 2 (c) and 5 (d).

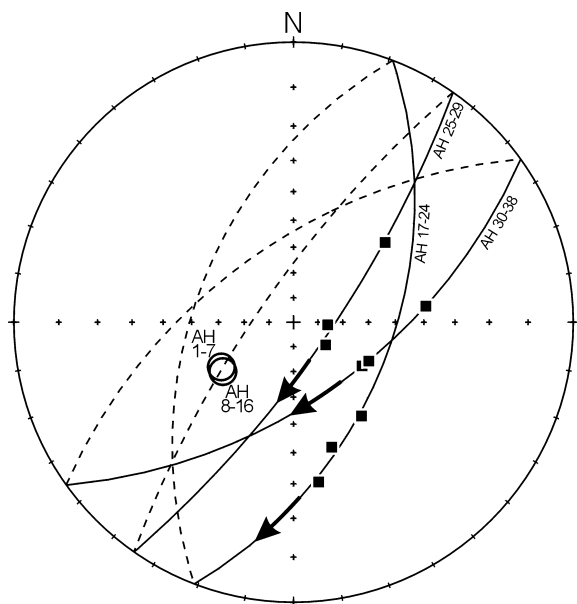


Fig. 8. Combination of stable end points and remagnetization circles for the five sites collected in locality 12. Stereographic projection. Larger circles are site-mean directions for the two sites yielding consistent directions (stable end points), solid squares are site mean directions in three subsequent demagnetization steps for the other three sites. Tectonic system, filled symbols are vectors pointing downward, open symbols, vectors pointing upward.

tions for the first two sites) and great circles (defined by the movement of the NRM vector during demagnetization) for the three other sites (method by McFadden and McElhinny, 1988), we obtain a statistically well-defined locality mean palaeomagnetic direction (Table 3).

In the *Lavanttal*, Ottnangian–Kárpátián sediments collected in the Granitztal subbasin (locality 5), a Badenian and a Sarmatian sediment from the Lavanttal basin proper yielded palaeomagnetic directions (Fig. 7a and b and Table 4) which are suitable for tectonic interpretation.

Locality 6 from the *Klagenfurt* basin behaves similarly to the marine sediments from the Lavanttal.

We also studied an undeformed magmatic dike from the *Gurktal block* (locality 20), which yielded K/Ar ages between 130 and 145 Ma (Kad. Balogh, 1998, written communication). The dike has good palaeomagnetic properties, the carrier of the NRM

is oxidized magnetite (Fig. 9) and the direction is statistically well-defined (Table 3). As we shall discuss later, this result is relevant to the model we propose to explain the palaeomagnetic results from the sediments of the intramontane basins.

## 5. Discussion

Miocene sediments in the intramontane basins of the Eastern Alps east of the Tauern window revealed counterclockwise (CCW) rotations, except localities 11 and 12 (Fig. 10a). The overall mean palaeomagnetic direction calculated from the locality mean directions of the former group (Tables 2–4, data in heavy print, the selection of either the tilt-corrected or the uncorrected data is explained partly in the previous chapter, partly in the further discussion) is statistically well-defined:  $D = 311^\circ$ ,  $I = 60^\circ$ ,  $k = 34$ ,  $\alpha_{95} = 7^\circ$ , based on 13 data. Compared with the stable European reference direction of corresponding age ( $D = 7^\circ$ ,  $I = 61^\circ$ , same as in Fig. 11), we can see a large and significant CCW rotation, which must have taken place very close to the stable European margin. Though the good statistical parameters would permit to interpret this rotation as a single, rigid block rotation of the whole western part of the study area, such interpretation is not plausible, basically because of space problems. We decided, therefore, to analyse the data further in order to find out if there are differences in the rotation angle between the studied basin systems on one hand, and between the declinations derived from older and younger strata, on the other hand.

In the western Noric depression (Figs. 10a and 11a, localities 7, 8, 9, 15) the grouping of the locality means is best when the mean directions of localities 7, 8 and 9 are in the tectonic, that of locality 15, in the geographic systems ( $D = 308^\circ$ ,  $I = 52^\circ$ ,  $k = 34$ ,  $\alpha_{95} = 16^\circ$ ). Since locality 15 is from pockets of clay in a conglomerate sequence, the unfavourable effect of the tilt correction does not necessarily mean secondary remanence: deposition in non-horizontal position is equally plausible.

The palaeomagnetic data from the Lavanttal basin (Figs. 10b and 11a, localities 2, 4, 5, 6) show close grouping before ( $D = 333^\circ$ ,  $I = 59^\circ$ ,  $k = 481$ ,

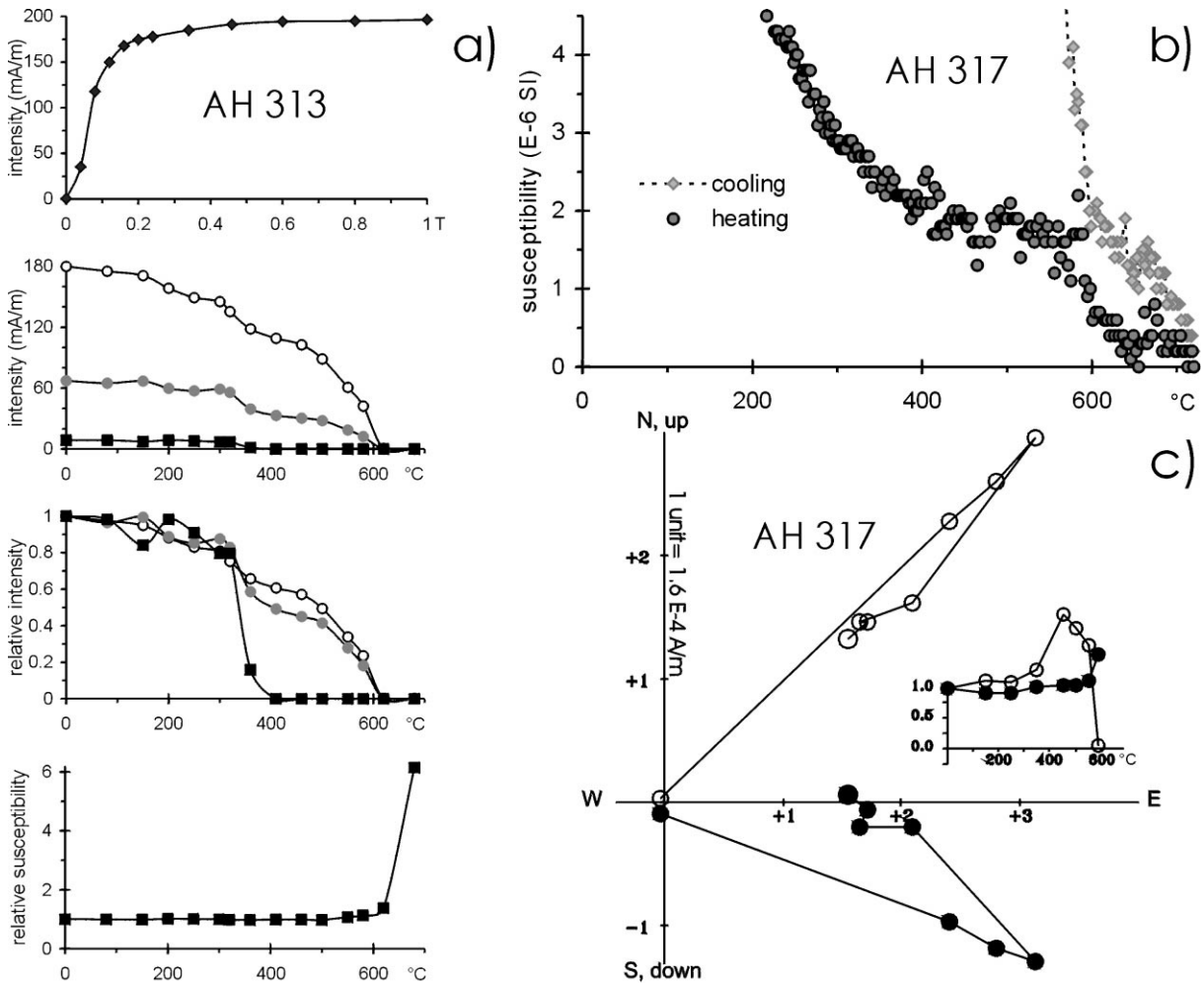
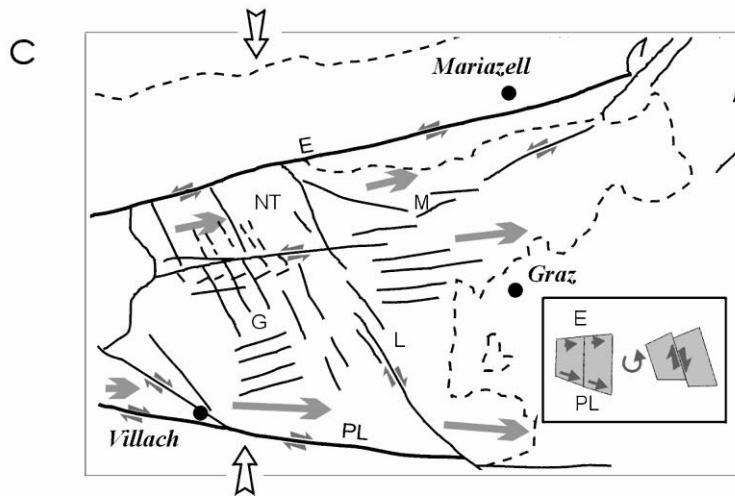
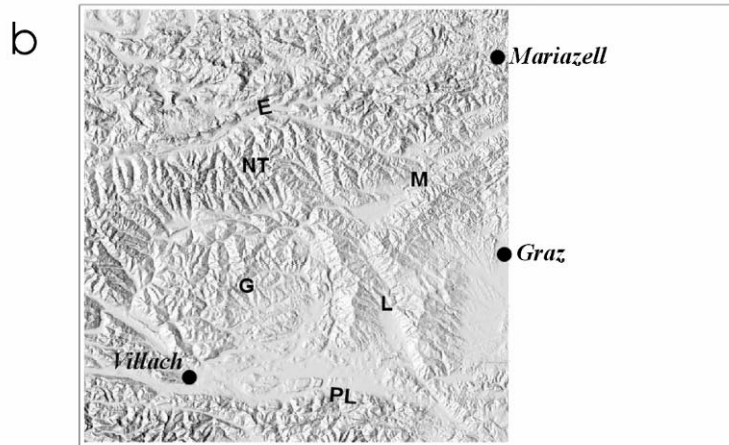
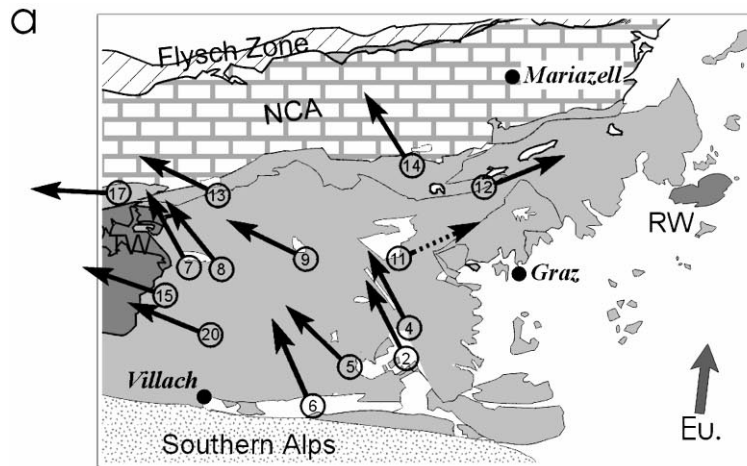


Fig. 9. The magmatic dike from locality 20. Left side: same as in Fig. 4, right side, top same as in Fig. 5, bottom, same as in Fig. 6.

$\alpha_{95} = 4^\circ$ ), but some scatter after bedding correction. Mechanically concluding, this means that the magnetic remanence was imprinted after sedimentation and tilting. However, locality 5 (Granitztal sub-basin) is different from the rest, being a terrestrial sediment, with less sensitive magnetic minerals (magnetite and hematite) to alteration than the others, and may carry a characteristic magnetization of pre-tilting age. If the overall palaeomagnetic mean direction is recalculated from the data in the geographic system of Table 4 without locality 5, we obtain  $D = 333^\circ$ ,  $I = 59^\circ$ ,  $k = 327$ ,  $\alpha_{95} = 7^\circ$ , which compared to the tilt corrected mean

of locality 5 (Table 4) shows a bit steeper inclination and ca.  $20^\circ$  less CCW rotation.

The results from the Ennstal basins (Figs. 10a and 11c, localities 13, 14, 17) are interpreted in terms of general CCW rotation. For localities 13 and 14 two magnetic components were identified: one interpreted to be of pre-, the other of post-tilting age, but nevertheless acquired before the rotation of the basins ended. The palaeomagnetic direction of locality 17 matches that of the others without the application of the tilt correction (part of the tilt may be primary, for the samples represent the matrix in a pebbly silt). The overall palaeo-



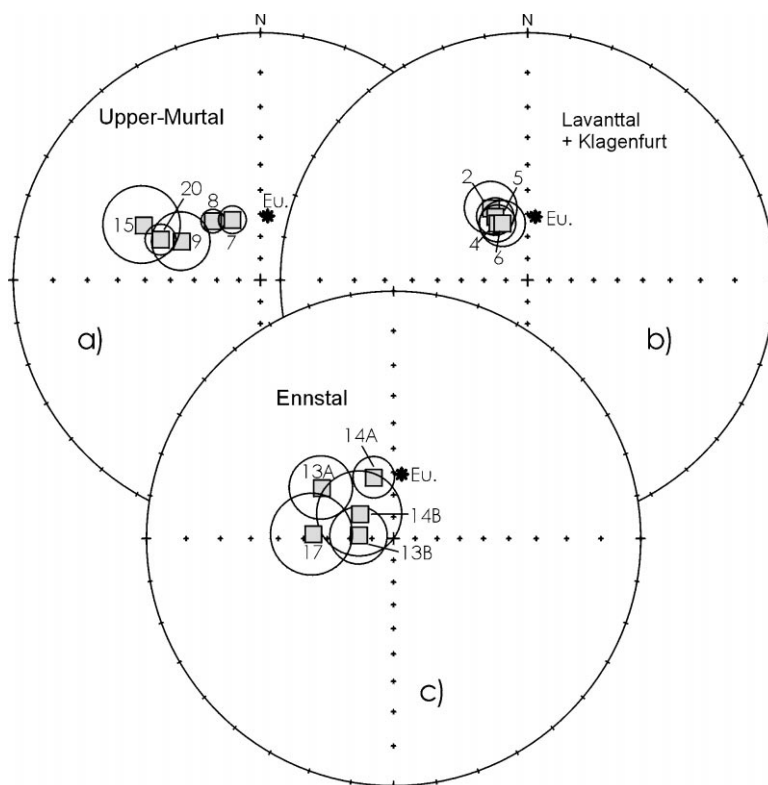


Fig. 11. Mean palaeomagnetic declinations, inclinations with  $\alpha_{95}$  on stereographic projection (for data refer to Tables 2–4). Overall mean palaeomagnetic direction for the western part of the Noric depression after tilt corrections is  $D=308^\circ$ ,  $I=+52^\circ$ ,  $k=25$ ,  $\alpha_{95}=19^\circ$ ; when locality 15 is taken before tilt correction the overall mean is  $D=306^\circ$ ,  $I=+55^\circ$ ,  $k=34$ ,  $\alpha_{95}=16^\circ$ . The overall palaeomagnetic directions for the Lavanttal and Klagenfurt basins before tilt corrections is  $D=333^\circ$ ,  $I=+59^\circ$ ,  $k=481$ ,  $\alpha_{95}=4^\circ$  without locality 5 is  $D=334^\circ$ ,  $I=+59^\circ$ ,  $k=327$ ,  $\alpha_{95}=7^\circ$ . The overall palaeomagnetic mean direction for the Ennstal basin is  $D=301^\circ$ ,  $I=+64^\circ$ ,  $k=25$ ,  $\alpha_{95}=16^\circ$ . For comparison, the stable European (Eu.) reference direction is shown calculated from the average of the 10 and 20 Ma old palaeomagnetic poles (Besse and Courtillot, 1991).

magnetic mean direction for the Ennstal basins is  $D=301^\circ$ ,  $I=64^\circ$ ,  $k=25$ ,  $\alpha_{95}=16^\circ$ .

When the overall mean palaeomagnetic directions of the three basin systems are compared, the less rotated declinations in the Lavanttal basin system and the Klagenfurt basin compared to the others is clear, while the inclinations are similar. Incidentally, it is the Lavanttal and Klagenfurt basins where the sediments are younger than in

the other basins and the magnetizations are even younger, being, with the likely exception of locality 5, of post-tilting age. Within the basin systems, the situation is similar: The older strata (localities 5, 9, 13, 14, 15, 17) exhibit declinations between  $273$  and  $315^\circ$ , while the declinations in the younger strata (localities 2, 4, 6, 7, 8) are between  $321$  and  $333^\circ$ .

This trend suggests that part of the CCW rota-

Fig. 10. Compilation of palaeomagnetic results and the main structures of the study area. (a) palaeomagnetic declinations for the successful localities (arrows with numbers) and the stable European reference direction (Eu, Besse and Courtillot, 1991). (b) Digital elevation model which mirrors the young age of the last displacements along major faults. (c) Interpretation of the palaeomagnetic data. E, Ennstal fault; M, Mur-Mürztal fault (Noric depression); L, Lavanttal fault; PL, Periadriatic Lineament; NT, Niedere Tauern; G, Gurktal Alps. The grey arrows show the direction of the extrusion, and are proportional to the displacement.

tions observed on the older strata is the result of a two-phase rotation. The earlier rotation may have occurred during sedimentation, that is, during the main phase of lateral tectonic extrusion, which, according to radiometric evidence (Dunkl and Demény, 1997; Frisch et al., 2000) and data from the sedimentary record in the Pannonian basin (Royden et al., 1982; Tari and Horváth, 1995; Dunkl et al., 1998) is bracketed between 18 and 13 Ma (Ottungian to Badenian).

The CCW rotations observed in the older strata of the intramontane basins are in line with previous pre-Tertiary results in the study area as well as with the result from the Nockalmsraße dike (locality 20). Earlier published magnetic vectors from Late Cretaceous sediments, forming the cover of

the Gurktal block and the Palaeozoic of Graz (Figs. 1 and 10), indicate CCW rotations up to  $60^\circ$  (Mauritsch and Becke, 1987; Agnoli et al., 1989). Permian redbeds in the Gurktal block also reveal counterclockwise rotations of  $50\text{--}70^\circ$  (Mauritsch et al., 1989; Mauritsch, 1993). Due to the good correspondence with the Miocene net rotation, it seems likely that the rotations observed on pre-Tertiary rocks (which are situated outside of the Miocene fault systems!) are essentially the product of Miocene tectonics.

Southeast of the study area, sediments of Karpatian and Badenian age in the Mura depression, in the Pohorje Mountains (Fig. 12d7) and in the Drauzug (Fig. 12d8) also exhibit moderate CCW rotations (Fodor et al., 1998). This shows

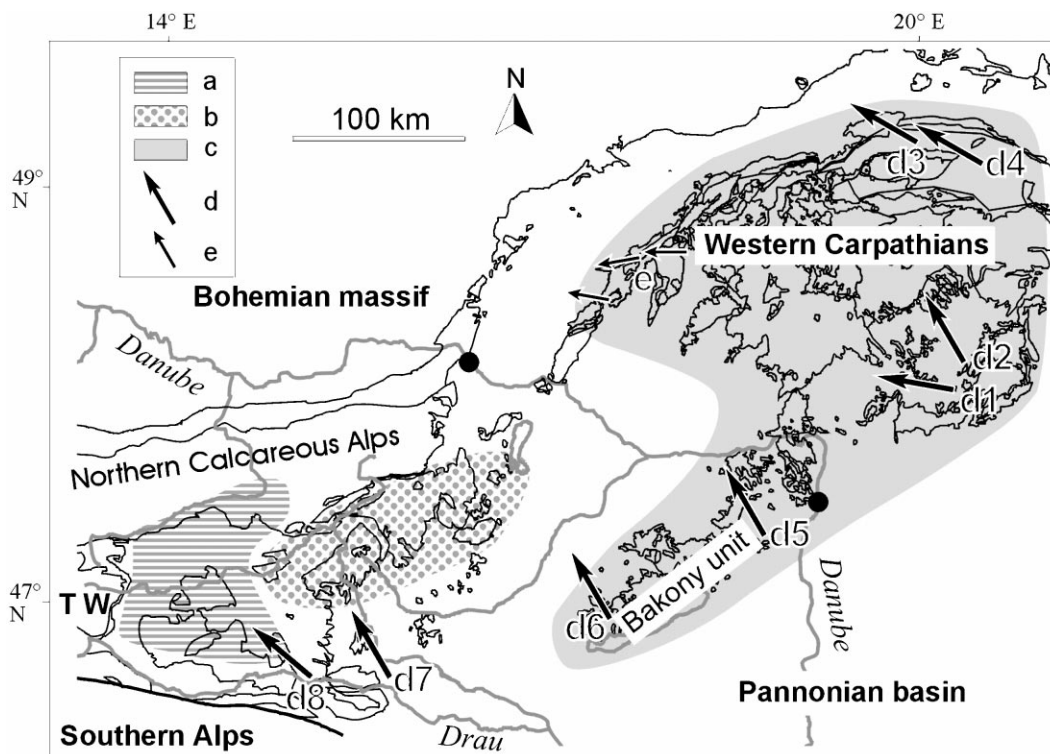


Fig. 12. Areas of Neogene rotations in the Eastern Alps and Western Carpathians. (a) Study area of this paper with syn- and post Middle Miocene CCW rotation; (b) transitional zone with Miocene CCW and CW rotations; (c) Western Carpathians and Bakony unit with Early–Middle Miocene CCW rotation; (d) overall mean palaeomagnetic declinations signifying Miocene rotations d1, d2: Márton and Márton (1996); d3, d4, Márton et al. (1998); d5, Márton (1986); d6, Márton and Márton (1983); d7, d8, Fodor et al. (1998); (e) locality mean palaeomagnetic declinations observed on Eocene rocks, interpreted as connected to Miocene rotations (Márton et al., 1996; Túnyi and Márton, 1996). Map contours are after Fuchs (1985).

that the CCW rotating area extends to the SE as far as the Periadriatic lineament.

The area with consistent CCW rotations is bordered in the east by the eastern segment of the Noric depression, where localities 11 and 12 with CW rotation are situated (Fig. 10a).

The area between the Periadriatic line (in the south) and the Ennstal fault system (in the north) exhibits characteristic fault patterns revealed by a digital elevation model (Fig. 10b). There is a pronounced NNW–SSE trending dextral fault array in the Gurktal and Niedere Tauern blocks (Fig. 10b and c), which are parallel to the Lavanttal fault. Along the western part of the Noric depression a complex interplay of these dextral faults and sinistral faults of the Murtal fault system define individual tectonic blocks of ca. 10 km diameter (Fig. 10b and c).

Based on the palaeomagnetic results and the fault pattern, we suggest that domino block rotations accommodated by dextral strike–slip along NNW–SSE trending faults occurred in the area between the Ennstal fault and the Periadriatic lineament. The basins were formed and sediment-filled during fault activity. The consistent dip of the strata in different basins (Tables 2 and 4) imply a uniform mechanism for the opening of the basins, related to domino block segmentation and rotation. The domino effect was the result of increasing eastward movement from north to south during extrusion (Fig. 10c). Faster eastward extrusion in the south is in line with the large-scale dextral displacement along the Periadriatic lineament in Miocene times (Frisch et al., 2000) and with stronger crustal extension as reflected by lower topographic elevations.

The domino mechanism probably did not account for the whole CCW rotation. After the termination of the extrusion process and thus of fault activity, CCW block rotation in the order of 30° (with respect to stable Europe) must have occurred.

East and south of our study area, Tertiary CCW rotations are known from several areas (Fig. 12), like the Bakony Mountains (d5 and d6) where post-Eocene rotation of ca. 35° was measured (Márton and Márton, 1983; Márton, 1986; Mauritsch and Márton, 1995); the North

Pannonian Palaeogene Basin (d1 and d2) where 80° net CCW rotation occurred as two separate events in the Miocene (Márton and Márton, 1996), the first (50°) took place in the time interval of 18.5–17.5 Ma, the second (30°) between 16 and 14 Ma (Márton and Pécskay, 1998); and the Western Carpathians (d3, d4 and e). Based on the palaeomagnetic constraints and the consideration of Jiricek (1979) on the termination of thrusting in the Carpathians we can conclude that the displacement seems to have migrated from NE to SW for in the Mura Depression as well as in our study area the rotations are definitely younger than the main rotation period of the Western Carpathians.

Surrounded by areas with Miocene CCW rotations, there is a poorly constrained area in the Alpine/Pannonian transition zone with a complex rotation pattern (Fig. 12). In this area lies our locality (11 and) 12, revealing clockwise rotation. In the same transition zone observations from the Rechnitz window (Márton et al., 1987; Mauritsch et al., 1991) and from metamorphics of the Palaeozoic of Graz (Flügel et al., 1980; Burgschwaiger et al., 1996) also indicate CW rotations; in contrast, two outcrops of mid-Miocene sediments close to the Rechnitz window and one outcrop in the metamorphic Bernstein window suggest moderate CCW rotation (Márton and Mauritsch, 1990).

The CCW rotations in the Eastern Alps, east of the Tauern window and in the northwestern Pannonian basin (Fig. 12d6, d5, d1 and d2) may be related to a corner effect around the spur of the Bohemian Massif. The Bohemian spur, protruding into the northeastern corner of the Eastern Alps (see Ratschbacher et al., 1991; Decker and Peresson, 1996; Reinecker and Lenhardt, 2000) was able to inhibit eastward motion during the extrusion process, thus creating an overall sinistral wrench corridor between the Bohemian massif and the Southern Alps. The transitional area with both CCW and CW rotations is positioned in the immediate front of the Bohemian spur. It may be a local complication in the overall motion pattern of tectonic blocks which is also reflected in the different fault pattern (Fig. 11c) west and east of the Lavanttal fault.

## 6. Conclusions

(1) With two exceptions, the intramontane basins of the Eastern Alps east of the Tauern window show counterclockwise rotation.

(2) There is a tendency of decreasing rotation angles with decreasing age of the sediments. This can be interpreted in terms of synsedimentary rotation during the process of lateral tectonic extrusion (ca. 18–13 Ma, Otnangian to Badenian), followed by ca. 30°, post-Sarmatian rotation.

(3) Rotation during lateral extrusion is explained by a domino block model. CCW rotation of the dominoes was accommodated by NNW–SSE trending dextral faults, which are conspicuous tectonic elements in the study area.

(4) The Miocene CCW rotation is a regional phenomenon in the area east of the Tauern window, between the Ennstal fault system and the Periadriatic lineament, and in the North Pannonian block. The regional CCW rotation may be related to a corner effect of the Bohemian spur during eastward block motion.

(5) Clockwise rotation of Miocene sediments in the eastern part of the Noric depression indicate that they may belong to a transition zone which is positioned in the immediate front of the Bohemian spur.

## Acknowledgements

The German Science Foundation financed this study in the frame of the Collaborative Research Centre 275. Further support was obtained by the OTKA Found (Hungarian National Scientific Found.) No. T022119. Kadosa Balogh carried out the radiometric age dating of the dike in this study. Gábor Imre made difficult drilling of soft sediments possible. Balázs Székely processed the digital elevation model for Fig. 10. All help is gratefully acknowledged.

## References

- Agnoli, F., Reisinger, J., Mauritsch, H.J., 1989. Paläomagnetische Ergebnisse aus zwei ostalpinen Gosau-Vorkommen (Oberkreide). *N. Jb. Geol. Paläont. Mh.* 1989, 265–281.
- Aric, K., Gutdeutsch, G., Klinger, W., Lenhardt, X., 1987. Seismological studies in the Eastern Alps. In: Flügel, W., Faupl, P. (Eds.), *Geodynamics of the Eastern Alps*. Deuticke, Wien, pp. 324–333.
- Beck-Mannagetta, P., 1952. Zur Geologie und Paläontologie des unteren Lavanttal. *Jb. Geol. Bundesanstalt Wien* 95, 1–102.
- Besse, J., Courtillot, V., 1991. Revised and synthetic apparent polar wander paths of the African, Eurasian, North American and Indian Plates, and true polar wander since 200 Ma. *J. Geophys. Res.* 96, B3, 4029–4050.
- Burgschwaiger, E., Mauritsch, H.J., Bierbaumer, M., Scholger, R., 1996. Miocene overprint in the Palaeozoic of Graz, Eastern Alps, Austria. *Geol. Carpath.* 47, 5–12.
- Christensen, J.N., Selverstone, J., Rosenfeld, J.L., DePaolo, D.J., 1994. Correlation by Rb–Sr geochronology of garnet growth histories from different structural levels within the Tauern Window, Eastern Alps. *Contrib. Mineral. Petrol.* 118, 1–12.
- Cliff, R.A., Droop, G.T.R., Rex, D.C., 1985. Alpine metamorphism in south-east Tauern Window, Austria: 2. Rates of heating, cooling and uplift. *J. Metamorphic Geol.* 3, 403–415.
- Decker, K., Peresson, H., 1996. Tertiary kinematics in the Alpine–Carpathian–Pannonian System links between thrusting transform faulting and crustal extension. In: Wessely, G., Liebl, W. (Eds.), *Oil and Gas in Alpidic Thrust Belts and Basins of Central and Eastern Europe*, Eur. Assoc. Petrol. Geol. Spec. Publ 5, 69–77.
- Dercourt, J., Zonenshayn, L.P., Ricou, L.E., Kazmin, V.G., Le-Pichon, X., Knipper, A.L., Grandjacquet, C., Sborshchikov, I.M., Boulin, J., Sorokhtin, O., Geysant, J., Lepvrier, C., Biju-Duval, B., Sibuet, J.C., Savostin, L.A., Westphal, M., Lauer, J.P., 1985. Presentation de 9 cartes paléogéographiques au 1/20000000 s'étendant de l'Atlantique au Pamir pour la période du Lias à l'Actuel. *Paléogéographie de la Tethys. Bull. Soc. Géol. France Paris, Huitième Série* 15, 636–652.
- Dunkl, I., Demény, A., 1997. Exhumation of the Rechnitz Window at the border of the Eastern Alps and Pannonian Basin during Neogene extension. *Tectonophysics* 272, 197–211.
- Dunkl, I., Grasemann, B., Frisch, W., 1998. Thermal effects of exhumation of a metamorphic core complex on hanging wall syn-rift sediments — an example from the Rechnitz Window, Eastern Alps. *Tectonophysics* 297, 31–50.
- Fisher, R., 1953. Dispersion on a sphere. *Proc. R. Soc. London, Ser. A* 217, 295–305.
- Flügel, H.W., Mauritsch, H.J., Heinz, H., Frank, W., 1980. Paläomagnetische und radiometrische Daten aus dem Grazer Paläozoikum. *Mitt. Österr. geol. Ges.* 71, 201–211.
- Fodor, L., Jelen, B., Márton, E., Skaberne, D., Car, J., Vrabec, M., 1998. Miocene–Pliocene tectonic evolution of the Slovenian Periadriatic fault — implications for Alpine–Carpathian extrusion models. *Tectonics* 17, 690–709.
- Frisch, W., 1979. Tectonic progradation and plate tectonic evolution of the Alps. *Tectonophysics* 60, 121–139.

- Frisch, W., Kuhlemann, J., Dunkl, I., Brügel, A., 1998. Palinspastic reconstruction and topographic evolution of the Eastern Alps during late Tertiary tectonic extrusion. *Tectonophysics* 297, 1–15.
- Frisch, W., Dunkl, I., Kuhlemann, J., 2000. Post-collisional large-scale extension in the Eastern Alps. *Geol. Soc. Am. Spec.* (in press).
- Fuchs, W., 1985. Grostektonische Neuorientierung in den Ostalpen und Westkarpaten unter Einbeziehung plattentektonischer Gesichtspunkte. *Jb. Geol. Bundesanstalt* 127 (4), 571–631.
- Harland, W.B., Armstrong, R.L., Cox, A.V., Craig, L.E., Smith, A.G., Smith, D.G., 1989. *A Geologic Time Scale*. Cambridge University Press, Cambridge, UK.
- Heinrich, M., 1978. Zur Geologie des Tertiärbeckens von Tamsweg mit kristalliner Umrahmung. *Jb. Geol. Bundesanstalt* Wien 120, 295–341.
- Irving, E., 1964. *Paleomagnetism and its Application to Geological and Geophysical Problems*. Wiley, New York. 399 pp.
- Jiricek, R., 1979. Tectogenetic development of the Carpathian arc in the Oligocene and Neogene. In: Mahel, M. (Ed.), *Tectonic Profiles through the West Carpathians*. Geol. Inst. D. Stur. Publ. Bratislava, pp. 205–214.
- Kempf, O., Schlunegger, F., Strunck, P., Matter, A., 1998. Paleomagnetic evidence for late Miocene rotation of the Swiss Alps: results from the north Alpine foreland basin. *Terra Nova* 10, 6–10.
- Kent, J.T., Briden, J.C., Mardia, K.V., 1983. Linear and planar structure in ordered multivariate data as applied to progressive demagnetization of paleomagnetic remanence. *Geophys. J. R. Astr. Soc.* 75, 593–621.
- Klaus, W., 1956. Mikrosporenhorizonte in Süd- und Ostkärnten. *Verh. Geol. Bundesanst.* 1956, 250–255.
- Lowrie, W., 1990. Identification of ferromagnetic minerals in a rock by coercivity and unblocking temperature properties. *Geophys. Res. Lett.* 17, 159–162.
- Márton, E., 1986. Paleomagnetism of igneous rocks from the Velence Hills and Mecsek Mountains. *Geophys. Trans.* 32, 83–145.
- Márton, E., Márton, P., 1983. A refined apparent polar wander curve for the Transdanubian Central Mountains and its bearing on the Mediterranean tectonic history. *Tectonophysics* 98, 43–57.
- Márton, E., Márton, P., 1996. Large scale rotations in Northern Hungary during Neogene as indicated by paleomagnetic data. *Paleomagnetism and Tectonics of the Mediterranean Region*, Morris, A., Tarling, D.H. (Eds.), *Geol. Soc. Spec. Publ.* 105, 155–173.
- Márton, E., Mauritsch, H.J., 1990. Structural application and discussion of a paleomagnetic post-Paleozoic data base for the Central Mediterranean. *Phys. Earth Planet. Interiors* 62, 46–59.
- Márton, E., Pécskay, Z., 1998. Complex evaluation of Paleomagnetic and K/Ar isotope data of the Miocene ignimbritic volcanics in the Bükk Foreland, Hungary. *Acta Geol. Hung.* 41 (4), 467–476.
- Márton, E., Mauritsch, H.J., Pahr, A., 1987. Paläomagnetische Untersuchungen in der Rechnitzer Fenstergruppe. *Mitt. Österr. geol. Ges.* 80, 185–205.
- Márton, E., Vass, D., Túnyi, I., 1996. Rotation of the south Slovak Paleogene and lower Miocene rocks indicated by paleomagnetic data. *Geol. Carpath.* 47, 31–41.
- Márton, E., Tokarski, A., Soták, J., 1998. Inner West Carpathian flysch: relation between paleomagnetic directions, principal susceptibility axes and sedimentary transport direction. *Carpathian–Balkan Geological Association, XVI Congress, 30 August–2 September, 1998*. Vienna, Austria. Abstracts.
- Márton, E., Mastella, L., Tokarski, A.K., 1999a. Large counterclockwise rotation of the Inner West Carpathian Paleogene Flysch — evidence from paleomagnetic investigation of the Podhale Flysch (Poland). *Phys. Chem. Earth (A)* 24 (8), 645–649.
- Márton, E., Pavelić, D., Tomljenović, B., Pamić, J., Márton, P., 1999b. First paleomagnetic results on Tertiary rocks from the Slavonian Mountains in the Southern Pannonian Basin, Croatia. *Geol. Carpath.* 50, 273–279.
- Mauritsch, H.J., 1993. Paleomagnetic data from the Paleozoic basement of the Alps. In: von Raumer, J.F., Neubauer, F. (Eds.), *Pre-Mesozoic Geology in the Alps*. Springer, Berlin, pp. 163–169.
- Mauritsch, H.J., Becke, M., 1987. Paleomagnetic investigations in the Eastern Alps and the southern border zone. In: Flügel, W., Faupl, P. (Eds.), *Geodynamics of the Eastern Alps*. Deuticke, Wien, pp. 282–308.
- Mauritsch, H.J., Márton, E., 1995. Escape models of the Alpine–Carpathian–Pannonian region in the light of paleomagnetic observations. *Terra Nova* 7, 44–50.
- Mauritsch, H.J., Reisinger, J., Agnoli, F., 1989. Paläomagnetische Ergebnisse aus dem Perm der Gurktaler Decke. *Carinthia II* 99, 383–390.
- Mauritsch, H.J., Márton, E., Pahr, A., 1991. Paleomagnetic investigations in highly metamorphosed rocks: Eastern Alps (Austria and Hungary). *Geophys. Trans.* 36, 49–65.
- McFadden, P.L., McElhinny, M.W., 1988. The combined analysis of remagnetization circles and direct observations in paleomagnetism. *Earth Planet. Sci. Lett.* 87, 161–172.
- Mottl, M., 1970. Die jungtertiären Säugetierfaunen der Steiermark, Südost-Österreich. *Mitt. Mus. Bergbau etc. Landesmuseums. Joanneum* 31 (1), 77–168.
- Papp, A., 1957. Landschnecken aus dem limnischen Tertiär Kärntens. *Carinthia II* 67, 85–94.
- Polesny, H., 1970. Beitrag zur Geologie des Fohnsdorf-Knittelfelder und Seckauer Beckens. Ph-D. Thesis Univ. Vienna.
- Ratschbacher, L., Frisch, W., Linzer, H.G., Merle, O., 1991. Lateral extrusion in the Eastern Alps, part 2: structural analysis. *Tectonics* 10, 257–271.
- Reinecker, J., Lenhardt, W., 2000. Present-day stress field and deformation in eastern Austria. *Geol. Rundschau*. (in press).
- Rögl, F., 1996. Stratigraphic correlation of the Parathethys Oligocene and Miocene. *Mitt. Ges. Geol. Bergbaustud. Österr.* 41, 65–73.
- Royden, L.H., Horváth, F., Burchfiel, B.C., 1982. Transform faulting, extension, and subduction in the Carpathian Pannonian region. *Geol. Soc. Am. Bull.* 93, 717–725.

- Sachsenhofer, R., 1988. Zur Inkohlung des Ennstal-Tertiärs—Sitzber. Österr. Akad. Wiss., math.-naturw. Kl., Abt. I Wien 197, 333–342.
- Schmid, M., 1974. Bericht über Untersuchungen im Tertiär des Lavanttales. Verh. Geol. Bundesanst. A 1974, 122–123.
- Tari, G., Horváth, F., 1995. Middle Miocene extensional collapse in the Alpine-Pannonian transition zone. In: Horváth, F., Tari, G., Bokor, C. (Eds.), Extensional Collapse of the Alpine Orogen and Hydrocarbon Prospects in the Basement and Basin Fill of the Western Pannonian Basin. In: Am. Assoc. Petrol. Geol. Int. Conf., Nice, Guidebook to Fieldtrip No. 6. Am. Assoc. Petrol. Geol. pp. 75–105.
- Tollmann, A., 1985. In: Geologie von Österreich vol. 2. Deuticke, Wien.
- Túnyi, I., Márton, E., 1996. Indications for large Tertiary rotation in the Carpathian–Northern Pannonian region outside of the North Hungarian Paleogene Basin. Geol. Carpath. 47 (1), 43–49.
- van der Voo, R., 1993. Paleomagnetism of the Atlantic, Tethys and Iapetus Oceans. Cambridge University Press, Cambridge. 411 pp.
- Vass, D., Túnyi, I., Márton, E., 1996. Young Tertiary rotations of the megaunit Pelso and the neighbour units of the West Carpathians. Slovak Geol. Mag. 96 (3), 363–367.
- Wagreich, M., Zetter, R., Bryda, G., Peresson, H., 1996. Das Tertiär von Hieflau (Steiermark): Untermiozäne Sedimentation in den Östlichen Kalkalpen. Zbl. Geol. Paläont. Teil 1 5/6, 633–645.
- Weber, L., Weiss, A., 1983. Bergbaugeschichte und Geologie der österreichischen Braunkohlevorkommen. Arch. Lagerst.forsch. Geol. Bundesanstalt Wien 4, 1–317.
- Zeilinger, G., Kuhlemann, J., Reinecker, J., Kázmér, M., Frisch, W., 1999. Das Tamsweger Tertiär im Lungau (Österreich): Fazies und Deformation eines intramontanen Beckens und seine regionale geodynamische Bedeutung. N. Jb. Geol. Pal. Abh. 214 (3), 537–568.